ISSN 1070-3284, Russian Journal of Coordination Chemistry, 2017, Vol. 43, No. 10, pp. 700–707. © Pleiades Publishing, Ltd., 2017.

A New Metalloligand Powerful in Forming Helical Coordination Polymers[1]

S. Z. Zhang[a], B. Yuan[a], Y. L. Lan[a], X. Z. Li[a, *], P. P. Hao[b, **], and L. N. Zhu[a]

[a] *Department of Chemistry, School of Science, Tianjin University, and Collaborative Innovation Center of Chemical Science and Engineering, Tianjin, 300072 P.R. China*

[b] *Department of Chemical Engineering, Ren'ai College of Tianjin University, Tianjin, 301636 P.R. China*

**e-mail: lixiaozeng321@tju.edu.cn*

***e-mail: haopeggy@tju.edu.cn*

Received October 5, 2016

Abstract—A new macrocyclic oxamido carboxylate metalloligand was designed and three heteronuclear coordination polymers of the metalloligand and metal nodes Cu^{2+}, Zn^{2+} and Cd^{2+} were prepared. X-ray single crystal analyses (CIF files CCDC nos. 1025722–1025724 for **I**–**III**) revealed that multiple favourable features endowed the metalloligand with a strong power to force the metal nodes to generate 1D helical coordination polymers. Thermogravimetric analyses showed that the complexes with Cu^{2+} and Zn^{2+} nodes exhibited moderate thermal stability. The three complexes were also characterized by IR spectra and PXRD.

Keywords: macrocyclic complex, metalloligand, crystal structure, helical coordination polymer

DOI: 10.1134/S1070328417100116

INTRODUCTION

Helical coordination polymers have intriguing structures, wide potential applications [1–17] and relevance with biological compounds of helical structures [1–4, 14–16, 18, 19]. Thus, the construction of such helices has attracted a lot of attention. Yet the controlled induction of helicity in preparing such assemblies is still challenging at the present stage [1–17, 20–22], and the difficulty in preparation has hindered the investigation of the helicity-dependent functions of this kind of compounds.

Much effort has been contributed to the selection and design of bridging ligands suitable for the construction of helical coordination polymers. Unfortunately, infinite 1D coordination helices of very few metal nodes have been documented for any single bridging ligand except the recently reported metalloligand NiL^1 (Scheme 1) to the best of our knowledge [1–3, 21, 22], implying that the formation of such structures is generally sensitive to the types of metal ions, that tuning their structural parameters and functions by varying metal nodes is rather difficult and that strong bridging ligands are highly demanded for their controlled assembly.

No helical coordination polymers and only two layered ones of NiL1 and the divalent metal node Cd^{2+} have been prepared although we have tried hard [23]. Perhaps new features should be incorporated into a bridging ligand similar to NiL1 for it to form helical coordination polymers with Cd^{2+} node. Herein a new metalloligand NiL^2 (Scheme 1) was designed and three helical coordination polymers, $\{[Cu(NiL2)(H_2O)_2] \cdot (CH_3)_2CHOH \cdot H_2O\}_n$ (**I**), $\{[Zn(NiL2)(H_2O)_3] \cdot CH_3OH \cdot 2H_2O\}_n$ (**II**) and $\{[Cd(NiL2)(H_2O)_3] \cdot 3H_2O\}_n$ (**III**), were prepared from it, hinting the powerfulness of the ligand to form such helices.

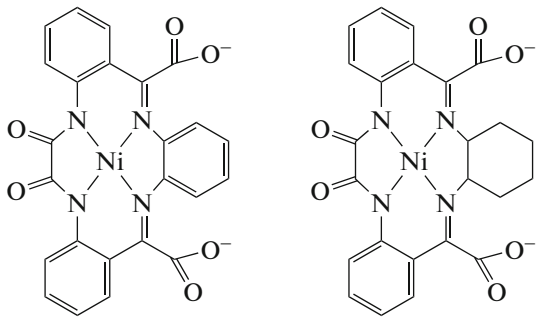

(NiL^1) (NiL^2)

Scheme 1.

EXPERIMENTAL

Materials and measurements. All starting materials and solvents were gained commercially and were used

[1] The article is published in the original.

as received. The preparation and ring opening of 1,1'-oxalylbisisatin were performed according to the literature method [23, 24]. Infrared spectra were recorded from KBr pellets on a BIO-RAD 3000 infrared spectrophotometer in the 400–4000 cm^{-1} region. Elemental analyses of C, H and N were achieved with a Perkin-Elmer 240 Elemental Analyzer. Powder X-ray diffraction (PXRD) data were obtained on a Riga D/max 2500v/pc X-ray powder diffractometer (CuK_α, λ = 1.5418 Å). Thermogravimetric (TG) analyses were conducted in the temperature range 31–800°C at a heating rate of 10°C/min under N_2 protection with a STA-409PC equipment.

Synthesis of NiL^2. A mixture of 1,1'-oxalylbisisatin (1.7420 g, 0.0050 mol) and a solution of NaOH (0.4000 g, 0.0100 mol) in water (50 mL) was stirred at 40°C for 2 h to give a yellow solution. To the solution was added triethylamine (1.49 mL, 0.0107 mol) and $Ni(OAC)_2 \cdot 4H_2O$ (1.2440 g, 0.0050 mol) under stirring. To the above solution was then added drop by drop a solution of 1,2-diaminocyclohexane (0.5400 g, 0.0047 mol; mixture of *trans*- (70%) and *cis*-1,2-diaminocyclohexane (30%)) in water (25 mL) within 2 h under stirring at 75°C. The resulting mixture was kept stirring for another 10 h at 80°C. The mixture was then cooled to room temperature and filtered under vacuum. The filtrate was evaporated by heating on a water bath of 60°C to afford an orange paste. The mixture of the paste and methanol (10 mL) was stirred for 30 min and then filtered under vacuum. The solid was dried in the air to afford an orange powder (1.7280 g). See also Scheme 2.

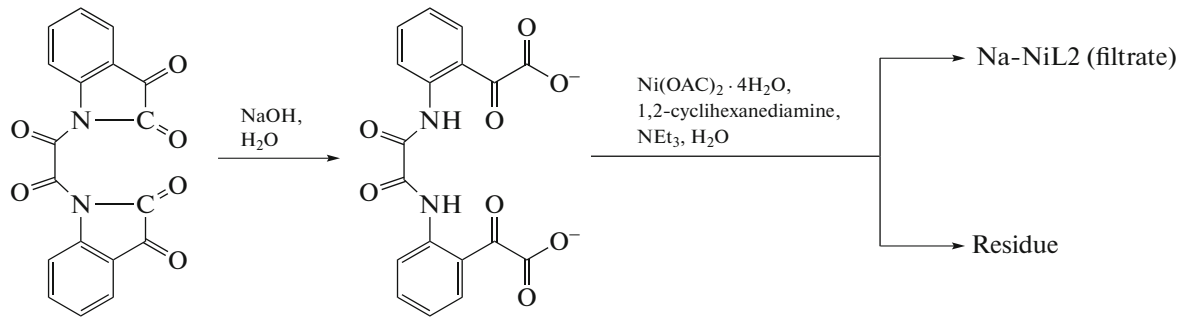

Scheme 2.

The orange powder contains NiL^2 according to the composition of **I**, **II**, and **III**. Pure Na-NiL^2 compound was not obtained and thus full characterization of the orange powder was not realized. However, the impurity did not hinder the synthesis of **I**–**III**.

Synthesis of I. A mixture of the orange powder (0.0620 g) from the NiL^2 preparation, $Cu(NO_3)_2 \cdot 3H_2O$ (0.0241 g, 0.0993 mmol), methanol (60 mL), water (60 mL) and isopropanol (60 mL) was stirred to form a pale yellow solution. The filtrate of the solution was then stored at room temperature for 20 days, and red crystals suitable for X-ray single crystal analysis were formed. The yield was 0.0320 g.

For $C_{27}H_{32}N_4O_{10}NiCu$

Anal. calcd., %:	C, 46.67;	H, 4.64;	N, 8.06.
Found, %:	C, 46.33;	H, 4.55;	N, 8.22.

IR (KBr; ν, cm^{-1}): 3428 m, 2920 m, 1606 s, 1586 s, 1558 s, 1443 m, 1373 s, 1315 m, 756 m.

Synthesis of II. A mixture of the orange powder (0.0460 g) from the NiL^2 preparation, $Zn(NO_3)_2 \cdot 6H_2O$ (0.0400 g, 0.1345 mmol), methanol (20 mL) and water (20 mL) was stirred to form a pale yellow solution. The filtrate of the solution was then stored at room temperature for 11 days, and red crystals suitable for X-ray single crystal analysis were formed. The yield was 0.0280 g.

For $C_{25}H_{28}N_4O_{12}NiZn$

Anal. calcd., %:	C, 42.83;	H, 3.93;	N, 8.01.
Found, %:	C, 42.90;	H, 4.07;	N, 7.92.

IR (KBr; ν, cm^{-1}): 3150 m, 2931 m, 1600 s, 1588 s, 1433 m, 1381 s, 1229 m, 749 s.

Synthesis of III. A mixture of the orange powder (0.0380 g) from the NiL^2 preparation, $CdCl_2 \cdot 2.5H_2O$ (0.0320 g, 0.1401 mmol), methanol (20 mL) and water (20 mL) was stirred to form a pale yellow solution. The filtrate of the solution was then stored at room temperature for 9 days, and red crystals suitable for X-ray single crystal analysis were formed. The yield was 0.0270 g.

For $C_{24}H_{30}N_4O_{12}NiCd$

Anal. calcd., %:	C, 39.08;	H, 4.10;	N, 7.60.
Found, %:	C, 39.44;	H, 4.02;	N, 7.69.

Table 1. Crystallographic data and structural refinement details for complexes **I**–**III**

Parameter	Value		
	I	**II**	**III**
Mr	694.82	704.62	737.63
Crystal system	Monoclinic	Monoclinic	Monoclinic
Space group	$P2_1/n$	$P2_1/n$	$P2_1/n$
a, Å	15.737(10)	15.444(17)	15.734(2)
b, Å	8.972(5)	9.006(10)	8.8889(11)
c, Å	20.073(12)	20.00(2)	20.031(3)
β, deg	96.207(6)	90.747(18)	90.783(9)
V, Å^3	2818 (3)	2782(5)	2801.2(7)
Z	4	4	4
ρ_{calcd}, g cm^{-3}	1.638	1.683	1.749
μ, mm^{-1}	1.488	1.611	1.501
F(000)	1436	1440	1496
Crystal size, mm	0.20 × 0.20 × 0.20	0.20 × 0.20 × 0.20	0.20 × 0.20 × 0.20
θ Range, deg	3.05–25.01	3.04–25.20	3.06–25.02
Limiting indices	$-18 \le h \le 18$, $-10 \le k \le 10$, $-23 \le l \le 23$	$-18 \le h \le 18$, $-10 \le k \le 10$, $-23 \le l \le 23$	$-18 \le h \le 18$, $-10 \le k \le 10$, $-23 \le l \le 23$
Reflections collected	23561	23390	22710
R_{int}	0.0901	0.1083	0.0771
Refinement parameters	405	388	379
GOOf on F^2	1.093	1.045	1.030
R_1, wR_2 ($I > 2\sigma(I)$)	0.0623, 0.1728	0.0558, 0.1365	0.0382, 0.0946
R_1, wR_2 (all data)	0.1070, 0.2185	0.0739, 0.1534	0.0420, 0.0994
S	1.093	1.045	1.030
Largest difference peak and hole, *e* Å^{-3}	1.310 and −1.084	1.029 and −0.614	1.040 and −0.771

IR (KB; ν, cm^{-1}): 3298 m, 2930 m, 1611 s, 1589 s, 1558 s, 1446 m, 1383 s, 1220 m, 751 m.

X-ray structure determinations. The diffraction data were collected at 293(2) K with a Bruker SMART CCD area detector using graphite-monochromated MoK_α radiation (λ = 0.71073 Å) with ω scans for I and II and with ω and φ scans for III. Absorption corrections were carried out utilizing SADBS routine [25]. The structures were solved by the direct methods [26] and refined by full-matrix least-squares refinements based on F^2 [27]. The crystallographic data are listed in Table 1 and selected bond lengths and angles are given in Table 2.

Crystallographic data for the structures have been deposited with the Cambridge Crystallographic Data Centre (CCDC nos. 1025722–1025724 for **I**–**III**; deposit@ccdc.cam.ac.uk, http://www.ccdc.cam.ac.uk).

RESULTS AND DISCUSSION

X-ray single crystal analyses showed that the cyclohexyl group of each NiL^2 ligand in **I**–**III** has the *R*-configuration at one chiral carbon and the *S*-configuration at the other (Fig. 1), indicating that the cyclohexyl groups in the NiL^2 ligands are all from *cis*-(1*R*,2*S*)-diaminocyclohexane.

The two coordinating tops of every NiL^2 ligand in all the three complexes adopt angular orientations. Angular exoditopic ligands are viable to generate helical coordination polymers [1–3, 28–32]. Each NiL^2 ligand in **I**–**III** chelates a node through the oxamido carbonyls and binds to another node *via* a carboxylate group, and consequently exhibits an asymmetric exoditopic coordination mode. This mode is also capable of leading to the formation of helical coordination polymers [1–3, 32–34]. Infinite right- (P) and left-handed (M) helical chains (Fig. 2) were formed with the arrangement of the NiL^2 ligands in head-to-tail

Table 2. Selected bond lengths (Å) and angles (deg) for complex **I**–**III***

Bond	*d*, Å	Bond	*d*, Å
		I	
Ni(1)–N(1)	1.875(4)	Ni(1)–N(2)	1.901(5)
Ni(1)–N(3)	1.874(5)	Ni(1)–N(4)	1.867(4)
Cu(1)–O(1)	1.968(4)	Cu(1)–O(2)	2.248(4)
Cu(1)–O(3)	1.978(4)	Cu(1)–O(7)	1.929(5)
Cu(1)–O(8)	1.944(5)		
		II	
Ni(1)–N(1)	1.897(4)	Ni(1)–N(2)	1.879(4)
Ni(1)–N(3)	1.869(4)	Ni(1)–N(4)	1.880(4)
Zn(1)–O(3)	2.088(4)	Zn(1)–O(4)	2.148(4)
Zn(1)–Oa(5)	2.157(4)	Zn(1)–O(7)	2.023(4)
Zn(1)–O(8)	2.075(4)	Zn(1)–O(9)	2.106(4)
		III	
Ni(1)–N(1)	1.883(3)	Ni(1)–N(2)	1.865(3)
Ni(1)–N(3)	1.856(3)	Ni(1)–N(4)	1.849(3)
Cd(1)–O(1)	2.265(3)	Cd(1)–O(2)	2.299(3)
Cd(1)–O^a(6)	2.292(3)	Cd(1)–O(7)	2.236(3)
Cd(1)–O(8)	2.278(4)	Cd(1)–O(9)	2.251(4)
Angle	ω, deg	Angle	ω, deg
		I	
N(1)Ni(1)N(2)	95.2(2)	N(1)Ni(1)N(4)	85.83(19)
N(3)Ni(1)N(1)	173.0(2)	N(3)Ni(1)N(4)	92.07(19)
N(4)Ni(1)N(2)	178.0(2)	N(3)Ni(1)N(2)	87.1(2)
O(1)Cu(1)O(3)	86.81(16)	O(1)Cu(1)O(2)	78.84(14)
O(1)Cu(1)O(8)	91.02(18)	O(1)Cu(1)O(7)	173.6(3)
O(2)Cu(1)O(7)	107.3(3)	O(2)Cu(1)O(3)	91.83(16)
O(3)Cu(1)O(7)	91.20(19)	O(2)Cu(1)O(8)	96.37(19)
O(7)Cu(1)O(8)	90.0(2)	O(3)Cu(1)O(8)	170.9(2)
		II	
N(1)Ni(1)N(2)	89.96(18)	N(1)Ni(1)N(3)	177.18(18)
N(1)Ni(1)N(4)	95.71(18)	N(3)Ni(1)N(2)	91.40(18)
N(4)Ni(1)N(2)	172.68(18)	N(3)Ni(1)N(4)	86.19(18)
O(3)Zn(1)O(4)	78.50(14)	O(3)Zn(1)O^a(5)	87.04(14)
O(3)Zn(1)O(7)	172.16(14)	O(3)Zn(1)O(8)	91.37(16)
O(3)Zn(1)O(9)	93.72(16)	O(4)Zn(1)O^a(5)	87.56(17)
O(4)Zn(1)O(7)	94.40(15)	O(4)Zn(1)O(8)	169.71(16)
O(4)Zn(1)O(9)	89.96(19)	O^a(5)Zn(1)O(7)	89.35(15)
O^a(5)Zn(1)O(8)	93.81(19)	O^a(5)Zn(1)O(9)	177.21(18)
O(7)Zn(1)O(8)	95.81(17)	O(7)Zn(1)O(9)	89.57(19)
O(8)Zn(1)O(9)	88.9(2)		
		III	
N(1)Ni(1)N(2)	95.81(14)	N(1)Ni(1)N(3)	176.12(14)
N(1)Ni(1)N(4)	86.87(14)	N(3)Ni(1)N(2)	86.50(13)
N(4)Ni(1)N(2)	172.43(14)	N(3)Ni(1)N(4)	91.23(14)
O(1)Cd(1)O(2)	72.73(9)	O(1)Cd(1)O^a(6)	85.83(11)
O(1)Cd(1)O(7)	168.97(10)	O(1)Cd(1)O(8)	95.41(12)
O(1)Cd(1)O(9)	92.97(13)	O(2)Cd(1)O^a(6)	86.44(12)
O(2)Cd(1)O(7)	98.32(11)	O(2)Cd(1)O(8)	88.65(16)
O(2)Cd(1)O(9)	165.62(13)	O^a(6)Cd(1)O(7)	87.19(11)
O^a(6)Cd(1)O(8)	174.34(16)	O^a(6)Cd(1)O(9)	94.22 (16)
O(7)Cd(1)O(8)	90.73(12)	O(7)Cd(1)O(9)	96.05(14)
O(8)Cd(1)O(9)	91.2(2)		

* Symmetry codes: [a] $1.5 - x$, $0.5 + y$, $1.5 - z$ (**II**); [a] $0.5 - x$, $-0.5 + y$, $0.5 - z$ (**III**).

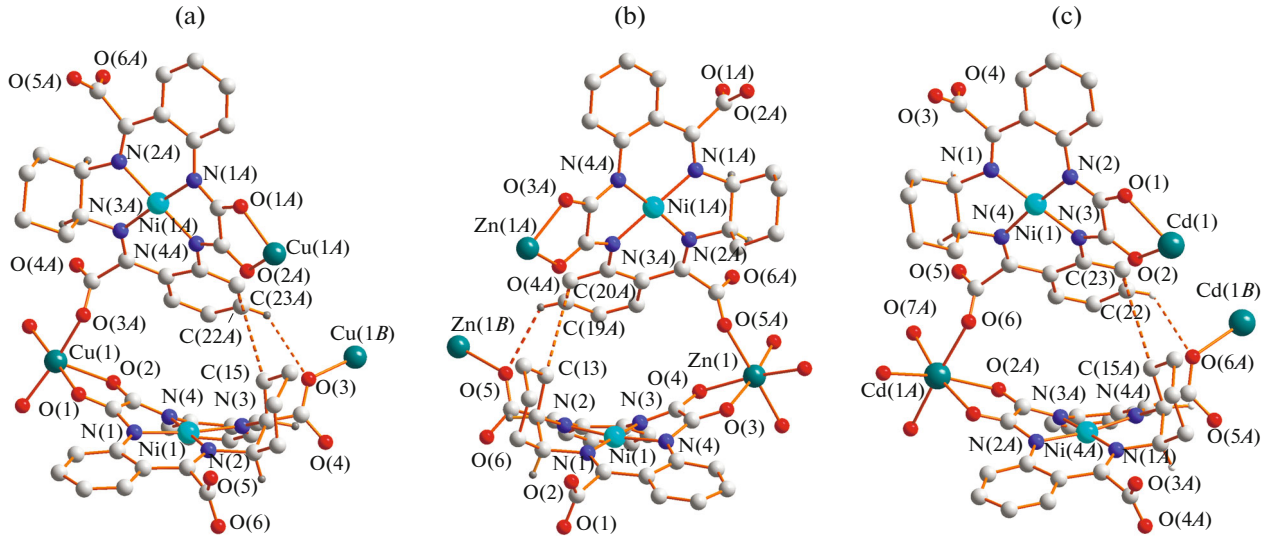

Fig. 1 Coordination environments of metal centers, metal-binding mode, "head-to-tail" arrangement and saddle shape of NiL^2, and C–H···O and hydrophobic interactions (dashed lines) between the two NiL^2 ligands binding to the same node in **I** (a), **II** (b) and **III** (c). Hydrogen atoms other than those on the chiral C atoms and involving in C–H···O H-bonds have been omitted for clarity.

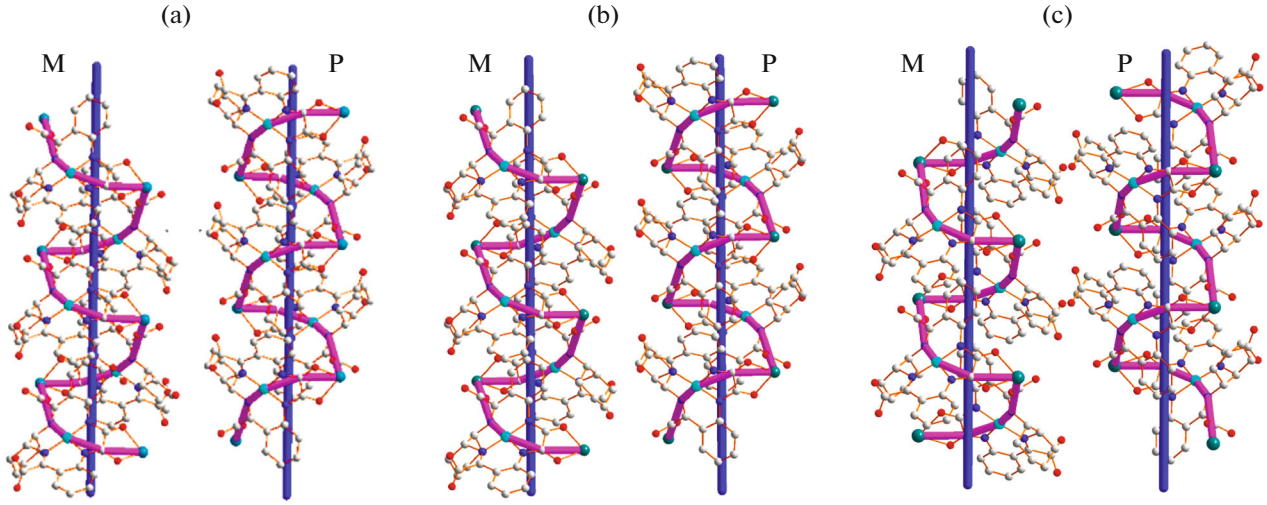

Fig. 2. Left- (M) and right-handed (P) helical chains in **I** (a), **II** (b) and **III** (c). Hydrogen atoms and coordinated solvent molecules have been omitted for clarity.

repeats, and the helical pitches are 8.972(5), 9.006(10) and 8.889(1) Å, respectively, for **I**, **II** and **III**.

The Ni centre of every NiL^2 ligand in **I**–**III** has a square planar N_4 coordination environment (Fig. 1). The largest deviations of the Ni and N atoms from the corresponding NiN_4 planes are less than 0.118 Å. The cyclohexyl and the two oxamido carbonyls of each NiL^2 ligand tilt on the same side of the NiN_4 plane, while the two phenyl rings tilt on the other side of this plane. As a result, the NiL^2 ligands assume saddle shapes. For each NiL^2 ligand, the dihedral angle between the plane determined by the oxamido group and the mean plane of the cyclohexyl is in the range of 76.7° to 86.1°, and that between the two phenyls falls into the much smaller range of 138.2°–140.5° (Table 3).

Every carboxylate group of all the NiL^2 ligands is caught between a phenyl and the cyclohexyl of the corresponding metalloligand. The dihedral angle between the plane defined by every carboxylate group and the NiN_4 plane of the corresponding NiL^2 ligand ranges from 57.6° to 72.0° (Table 3). In addition, the carboxylate groups bind to the rigid macrocycles of the NiL^2 ligands. Therefore, the carboxylate groups present lit-

Table 3. Dihedral angles (deg) between mean planes of every NiL^2 ligand in **I**–**III**

Complex	Angle 1[a]	Angle 2[b]	Angle 3[c]
I	76.7(2)	138.6(2)	57.6(2), 72.0(5)
II	83.9(2)	138.2(2)	61.7(2), 70.3(5)
III	86.1(1)	140.5(1)	63.9(2), 70.9(3)

[a] The dihedral angle between the planes defined by the oxamido group and the cyclohexyl ring opposite to it.
[b] The dihedral angle between the two phenyl rings opposite to each other.
[c] The dihedral angle between the plane determined by every carboxylate group and the NiN_4 plane.

tle freedom of bending and rotation. This fact, the shape similarity of the NiL^2 ligands together with the small ranges of the above dihedral angles clearly shows that NiL^2 has high rigidity. Rigid bridging ligands are certainly superior to flexible ones in maintaining the shapes supporting the formation of helical coordination polymers in the assembly reactions.

Each metal node in **I**–**III** was coordinated by the two oxamido O atoms of a NiL^2 ligand and a carboxylate O atom of another NiL^2 ligand (Fig. 1). The coordination sphere of each metal node in **I** is completed by two aqua ligands, and that in **II** and **III** by three aqua ligands. Thus the nodes in **I** adopt distorted square pyramidal coordination geometries and those in **II** and **III** have distorted octahedral ones.

The two oxamido O atoms and the carboxylate O atom binding to the same metal node and the node itself in each of **I**–**III** constitute a triangular pyramid geometry (Fig. 1). The relative positions of the four atoms should be favourable to the NiL^2 ligands adopting positions and orientations supporting the formation of the helical chains. A helical coordination polymer of NiL^1 bridging ligand and Zn^{2+} node was obtained in the existence of aqua coligands [23], but two 1D non-helical ones with the same bridging ligand and metal node were formed in the existence of *N*,*N*-dimethylacetamide and *N*,*N*-dimethylformamide coligands [35]. The three coordinating O atoms of the NiL^1 ligands and the Zn^{2+} node in the above helix take the same disposition as that in **I**–**III**, but the three coordinating O atoms of the NiL^1 ligands hold three positions coplanar with the Zn^{2+} node in each of the two non-helical 1D complexes. The above conditions of the Zn^{2+} compounds support that the triangular pyramid geometry determined by the three coordinating O atoms and the metal node favours the formation of helical chains and that the foregoing coplanar arrangement of the donor atoms and metal node disfavours the production of such helices.

In each helical coordination polymer of the NiL^1 bridging ligand, the two oxamido O atoms and the carboxylate O atom binding to the same metal node and the node itself take up relative positions favouring the formation of the helix, similar to the cases of **I**–**III**. Such favourable positions were supported by the π···π interactions between the NiL^1 ligands [21–23]. On the contrary, the number of atom-to-atom distances less than 3.80 Å between the π-systems of the two NiL^2 ligands binding to the same metal node (Table 4) indicates that support from π···π interactions is significantly less for **I**, is very little for **II** and **III**. Such shortage of π···π interactions in the helical chains should be related to the steric hindrance from the cyclohexyl group of the NiL^2 ligand in **I**–**III**. Some atom-to-atom distances between the cyclohexyl of the NiL^2 ligand chelating the node and a phenyl of the other NiL^2 ligand binding to the same node in each of **I**–**III** (Fig. 1, Table 4) are short, revealing not only the foregoing steric hindrance but also hydrophobic interactions. The hydrophobic interactions should favour the above arrangement of the two NiL^2 ligands. Besides, the C–H···O H-bond between the two NiL^2 ligands binding to the same node (Fig. 1, Table 5) should also support the above disposition of the NiL^2 ligands.

The bands in the 3500–3000 cm^{-1} range of the IR spectra are absorptions originated from the isopropanol molecule in **I**, the methanol molecule in **II** and the water molecules in all the three complexes. Compound **I**, **II** and **III** showed a very strong band at 1606, 1600 and 1611 cm^{-1}, respectively, which should includes the absorptions of both the oxamido C=O groups and the coordinating carboxylate groups [36–38]. The bands at 1586 cm^{-1} for **I**, 1588 cm^{-1} for **II** and 1589 cm^{-1} for **III**, which have little relevance to the types of the nodes, are attributed to ν(C=N) [36].

TGA plots of polycrystalline **I** and **II** are given in Fig. 3. Compound **I** began to lose weight at ~81°C, and 21.20% of its weight was lost up to ~268°C. Such a mass reduction approximately corresponds to the loss of three water molecules, an isopropanol molecule and a carboxylate group (calcd. 22.19%). More detailed mass loss steps in the temperature range of 81–268°C cannot be assigned. Almost no mass change occurred in the temperature range of 268–340°C. Then compound **I** decomposed further when the temperature went higher. The mass decrease of compound II was 6.54% from 77 to 143°C, being attributed to the loss of a methanol molecule and a water molecule (calcd. 7.10%). The mass was nearly constant from 143 to 152°C. In the temperature range of 152–395°C, the weight reduction was 14.50%, which may be due to the loss of the other four water molecules and a carboxyl-

Table 4. Short atom-to-atom distances (Å) between the two NiL^2 ligands binding to the same metal node in a helical chain of **I**–**III***

I			
C(24)···C(21)[a]	3.710 (8)	C(1)···C(20)[a]	3.624(7)
N(4)···C(21)[a]	3.705(7)	C(15)···C(22)[a]	3.649(1)
O(2)···C(20)[a]	3.433(7)	C(15)···C(23)[a]	3.598(1)
II			
O(4)···C(17)[a]	3.638 (8)	C(13)···C(19)[a]	3.538(9)
C(13)···C(20)[a]	3.536(9)		
III			
C(20)···O(2)[a]	3.701(5)	C(22)···C(15)[a]	3.574(6)
C(23)···C(15)[a]	3.608(6)		

* Symmetry codes: [a]$1.5 - x, -0.5 + y, 0.5 - z$ (**I**); $1.5 - x, 0.5 + y, 1.5 - z$ (**II**); $0.5 - x, 0.5 + y, 0.5 - z$ (**III**).

Table 5. Geometric parameters of the C–H···O hydrogen bond between the two NiL^2 ligands binding to the same metal node in a helical chain of **I**–**III**

Compound	Distance, Å			Angle C–H···O, deg
	C–H	H···O	C···O	
I	0.931	2.622	3.418(7)	143.9
II	0.930	2.645	3.354(7)	133.5
III	0.929	2.584	3.315(5)	135.9

ate group (calcd. 15.91%). Then appeared the second temperature range (395–418°C) with almost no mass loss. Heating the sample to higher temperatures led to further decomposition of the compound.

The measured PXRD patterns of **I**–**III** match well with the corresponding ones simulated from the data of the X-ray single crystal diffraction, revealing the uniformity of every sample with the corresponding single crystal.

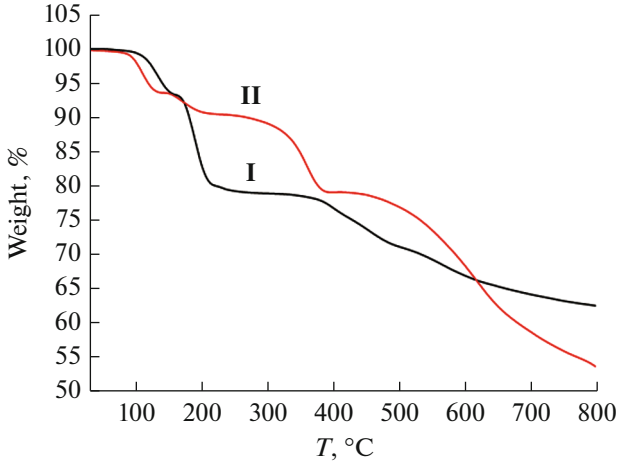

Fig. 3. TGA plots of compounds **I** and **II**.

The self-assembly of **I**–**III** manifests that NiL^2 is powerful in compelling diverse metal ions to form helical coordination polymers and that the introduction of cyclohexyl into NiL^2 enable it to generate the 1D helix with Cd^{2+} nodes rather 2D layers like those from NiL^1. It can be inferred that a comprehensive strategy employing a bridging ligand with multiple favourable features would be efficient to produce 1D helical coordination polymers and that the fine tune of the structures of bridging ligands can increase their adaptability to different metal ions in forming such helical complexes.

ACKNOWLEDGMENTS

This work was supported by the National Natural Science foundation of China (grant no. 21371130).

REFERENCES

1. Han, L. and Hong, M.C., *Inorg. Chem. Commun.*, 2005, vol. 8, no. 4, p. 406.
2. Zheng, X.D. and Lu, T.B., *CrystEngComm*, 2010, vol. 12, p. 324.

3. Leong, W.L. and Vittal, J., *J. Chem. Rev.*, 2011, vol. 111, no. 2, p. 688.
4. Yuan, G.Z., Zhu, C.F., Liu, Y., and Cui, Y., *J. Am. Chem. Soc.*, 2009, vol. 131, no. 30, p. 10452.
5. Zhang, J.P., Qi, X.L., He, C.T., and Chen, X.M., *Chem. Commun.*, 2011, vol. 47, no. 14, p. 4156.
6. Stephenson, A. and Ward, M.D., *RSC Adv.*, 2012, vol. 2, no. 29, p. 10844.
7. Ding, S., Gao, Y.F., Ji, Y.F., and Liu, Z.L., *CrystEngComm*, 2013, vol. 15, no. 28, p. 5598.
8. Sun, Y.Q., Deng, S., Liu, Q., and Chen, Y.P., *Dalton Trans.*, 2013, vol. 42, no. 29, p. 10503.
9. Sawada, T., Matsumoto, A., and Fujita, M., *Angew. Chem. Int. Ed.*, 2014, vol. 53, no. 28, p. 7228.
10. Bhattacharyya, A. and Chattopadhyay, S., *RSC Adv.*, 2015, vol. 5, no. 24, p. 18252.
11. Fang, W.Z., Wang, Y.P., Wang, Y.F., et al., *RSC Adv.*, 2015, vol. 5, no. 24, p. 8996.
12. Dubey, M., Kumar, A., and Pandey, D.S., *Chem. Commun.*, 2014, vol. 50, no. 14, p. 1675.
13. Gao, E.Q., Yue, Y.F., Bai, S.Q., et al., *J. Am. Chem. Soc.*, 2004, vol. 126, no. 5, p. 1419.
14. Roth, A., Koth, D., Gottschaldt, M., and Plass, W., *Cryst. Growth Des.*, 2006, vol. 6, no. 12, p. 2655.
15. Joarder, B., Chaudhari, A.K., and Ghosh, S.K., *Inorg. Chem.*, 2012, vol. 51, no. 8, p. 4644.
16. Shinozaki, Y., Richards, G., Ogawa, K., et al., *J. Am. Chem. Soc.*, 2013, vol. 135, no. 14, p. 5262.
17. Thio, Y., Yang, X., and Vittal, J.J., *Dalton, Trans.*, 2014, vol. 43, no. 9, p. 3545.
18. Yu, F.T., Penner-Hahn, J.E., and Pecoraro, V.L., *J. Am. Chem. Soc.*, 2013, vol. 135, no. 48, p. 18096.
19. Yashima, E., Maeda, K., Iida, H., et al., *Chem. Rev.*, 2009, vol. 109, no. 11, p. 6102.
20. Li, C.P., Wu, J.M., and Du, M., *Inorg. Chem.*, 2011, vol. 50, no. 19, p. 9284.
21. Li, X.Z., Hao, P.P., Wang, D., and Zhu, L.N., *CrystEngComm*, 2013, vol. 15, no. 15, p. 2800.
22. Wang, H.L., Wu, S.B., Shi, X.M., et al., *J. Inorg. Organomet. Polym.*, 2015, vol. 25, no. 4, p. 730.
23. Li, X.Z., Hao, P.P., Wang, D., et al., *CrystEngComm*, 2012, vol. 14, no. 2, p. 366.
24. Black, D.S.C. and Moss, G.I., *Aust. J. Chem.*, 1987, vol. 40, no. 1, p. 129.
25. Sheldrick, G.M., *SADABS, Program for Empirical Absorption Correction of Area Detector Data*, Göttingen: Univ. of Göttingen, 1996.
26. Sheldrick, G.M., *SHELXS-97, Program for the Solution of the Crystal Structures*, Göttingen: Univ. of Göttingen, 1990.
27. Sheldrick, G.M., *SHELXL-97, Program for the Refinement of the Crystal Structures*, Göttingen: Univ. of Göttingen, 1997.
28. Kim, H.J., Lee, E., Park, H.S., and Lee, M., *J. Am. Chem. Soc.*, 2007, vol. 129, no. 36, p. 10994.
29. Li, X.Z., Li, M., Li, Z., et al., *Angew. Chem. Int. Ed.*, 2008, vol. 47, no. 34, p. 6371.
30. Adarsh, N.N. and Dastidar, P., *Chem. Soc. Rev.*, 2012, vol. 41, no. 8, p. 3039.
31. Wei, K., Ni, J., Min, Y., et al., *Chem. Commun.*, 2013, vol. 49, no. 74, p. 8220.
32. Sun, W., Zhang, C., Ma, H., et al., *Dalton Trans.*, 2014, vol. 43, no. 43, p. 16322.
33. Chen, X.D., Dub, M., and Mak, T.C.W., *Chem. Commun.*, 2005, no. 35, p. 4417.
34. He, W.W., Yang, J., Yang, Y., et al., *Dalton Trans.*, 2012, vol. 41, no. 32, p. 9737.
35. Kong, X.J., Li, X.Z., and Zhu, L.N., *J. Coord. Chem.*, 2012, vol. 65, no. 24, p. 4315.
36. Gao, E.Q., Tang, J.K., Liao, D.Z., et al., *Helv. Chim. Acta*, 2001, vol. 84, no. 4, p. 908.
37. Warrier, A.V.R. and Narayanan, P.S., *Spectrochim. Acta*, 1967, vol. 23, no. 4, p. 1061.
38. Tasdemir, E., Ozbek, F.E., Sertcelik, M., et al., *J. Mol. Struct.*, 2016, vol. 1119, p. 472.